AIP | Applied Physics Letters

Detection of in-depth helical spin structures by planar Hall effect

Ali C. Basaran, R. Morales, S. Guénon, and Ivan K. Schuller

Citation: Applied Physics Letters **106**, 252404 (2015); doi: 10.1063/1.4923095
View online: http://dx.doi.org/10.1063/1.4923095
View Table of Contents: http://scitation.aip.org/content/aip/journal/apl/106/25?ver=pdfcov
Published by the AIP Publishing

Detection of in-depth helical spin structures by planar Hall effect

Ali C. Basaran,[1,a)] R. Morales,[2,3] S. Guénon,[1,b)] and Ivan K. Schuller[1]
[1]*Department of Physics and Center for Advanced Nanoscience, University of California San Diego, La Jolla, California 92093, USA*
[2]*Department of Chemical-Physics & BCMaterials, University of the Basque Country UPV/EHU, Leioa 48940, Spain*
[3]*IKERBASQUE, Basque Foundation for Science, Bilbao 48011, Spain*

(Received 16 April 2015; accepted 16 June 2015; published online 23 June 2015)

We developed a method to determine the magnetic helicity and to study reversal mechanisms in exchange biased nanostructures using Planar Hall Effect (PHE). As a test case, we use an in-depth helical spin configuration that occurs during magnetization reversal in exchange coupled Ni/FeF_2 heterostructures. We show the way to induce and determine the sign of the helicity from PHE measurements on a lithographically patterned cross. The helicity sign can be controlled by the angle between the externally applied magnetic field and a well-defined unidirectional anisotropy axis. Furthermore, the PHE signal reveals complex reversal features due to small deviations of the local unidirectional anisotropy axes from the crystallographic easy axis. The simulations using an incomplete domain wall model are in excellent agreement with the experimental data. These studies show that helical spin formations in nanomagnetic systems can be studied using laboratory-based magnetotransport. © *2015 AIP Publishing LLC*.
[http://dx.doi.org/10.1063/1.4923095]

Harnessing the average spin state of charge carriers produced new physics as well as unique technologies.[1,2] An important advance would be the formation and control of the spatial dependence of complex spin structures in nanomagnetic systems.[3] For example, magnetic helicity can be used to add right or left-handedness in thin films to engineer interesting structures. Such in-depth helical spin structures can be formed in low anisotropy magnetic films in proximity with a high anisotropy ferromagnet[4] or an antiferromagnet.[5] However, the detection of depth dependent magnetic profiles[6–8] or helical spin formations[9,10] is not trivial. Anisotropic magnetoresistance (AMR) measurements are insensitive to the direction of transverse magnetic moments,[11,12] and conventional microscopy techniques are resolution and depth limited. The magnetic moment reversal of large area samples can be studied using longitudinal and transverse magneto-optical Kerr effect[13] or vector magnetometry.[14] However, investigating the magnetization reversal process in nanomagnetic systems, such as wires and junctions, is challenging because the magnetic signal from such structures is weak.

On the other hand, the Planar Hall Effect (PHE)[15] obtained from the transverse voltage is extremely sensitive to changes in the local spin configuration and can be used to map out such complex spin formations. PHE is mostly preferred in sensor technologies[16–18] due to its directional sensitivity and low background voltage.[19] PHE was used to study the magnetization reversal in exchange biased (Ga,Mn)As/MnO heterostructures[20] and to determine the chirality of a vortex in a magnetic nanodot.[21]

In this letter, we present a PHE based technique, which reveals the helicity and details of complex reversal mechanisms in exchange-coupled Ni/FeF_2 cross junctions. Epitaxial, insulating, and antiferromagnetic (AFM) FeF_2 films induce a well-defined unidirectional anisotropy axis below the AFM Néel temperature (78 K) on ferromagnetic (FM) Ni overlayers, which develop a helical spin structure during the reversal. As a consequence, small angular variations around the unidirectional anisotropy axis change the helicity and produce large, opposite PHE signals. Furthermore, the PHE reveals complex reversal features due to small deviations of the local unidirectional anisotropy axes from the crystallographic easy axis (EA). These magnetic field and angular dependences of the PHE were simulated using an incomplete domain wall model. Experimental and simulated data are in excellent agreement for all geometries and magnetic fields.

In order to obtain the cleanest possible interface, the Ni/FeF_2 bilayers were grown without breaking vacuum on a 5 mm × 10 mm (110) MgF_2 substrate using electron beam evaporation at a base pressure of 1×10^{-7} Torr. 100 nm FeF_2 and 10 nm Ni were deposited with a rate of 1 Å/s at 300 °C and 150 °C, respectively. During the deposition, the maximum pressure of the chamber was kept below 6×10^{-7} Torr. Two separate samples were prepared simultaneously; one as a reference for exchange bias studies and the other used to fabricate a cross device for PHE measurements. Four separate devices, from two different depositions were investigated. The cross junction was fabricated by standard photolithography and etching. Ar ion milling was used to etch only the Ni layer to obtain ∼1 μm square cross-junction (inset of Fig. 1(b)). The junction size was kept large enough to avoid possible shape anisotropy effects. This was followed

a)Author to whom correspondence should be addressed. Electronic mail: abasaran@physics.ucsd.edu
b)Present address: Physikalisches Institut and CQ Center for Collective Quantum Phenomena and their Applications in LISA+, Eberhard-Karls-Universität Tübingen, Auf der Morgenstelle 14, D-72076 Tübingen, Germany.

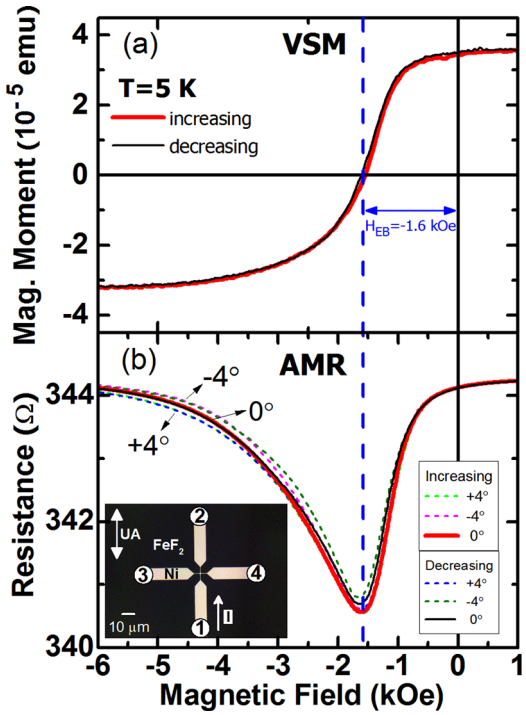

FIG. 1. Comparison of two measurement techniques at 5 K after 50 Oe field cooling; (a) magnetization measurement of a reference film (the applied field was swept along the unidirectional anisotropy axis (UA)). (b) AMR signal of the cross junction obtained using two contacts (V_{12}) at 0°, +4°, and −4°. Thin black and thick red lines correspond to decreasing and increasing field sweeps at 0°, respectively, and dashed lines correspond to ±4° for AMR. (Inset) Microscope image of lithographically patterned cross junction and corresponding measurement geometry. Blue dashed line indicates the exchange bias field.

by a second photolithography step to make electrical contacts for transport measurements. Top (Ti (10 nm)/Au (90 nm)) contacts were deposited in a sputtering chamber with 2×10^{-7} Torr base pressure with a constant 4 mTorr Ar flow during deposition. To remove any photoresist residue, 3 min of argon ion milling was performed *in-situ* prior to Ti deposition. PHE measurements were performed by applying ∼0.1 mA DC along the unidirectional anisotropy axis, between contacts 1 and 2, and measuring voltage between contacts 3 and 4 (inset of Fig. 1(b)).

The basic structural and magnetic properties of a reference FeF_2 (100 nm)/Ni (10 nm) bilayer were studied first. The X-ray diffraction (not shown) implies that the FeF_2 and Ni layers grow epitaxially and textured, respectively. Magnetization measurements using a vibrating sample magnetometer (VSM) confirm that the magnetic easy axis of the Ni layer coincides with the [001] direction of the AFM FeF_2, the unidirectional anisotropy axis below the Néel temperature. The typical 300 K square hysteresis loop has a remnant ratio of $M_r/M_s = \sim 1$ and coercive field of 30 Oe (with M_r and M_s remanent and saturation magnetization, respectively). Afterwards, the sample was cooled in 50 Oe field to 5 K at 4 K/min cooling rate. Fig. 1(a) shows the magnetic hysteresis loop at 5 K obtained from increasing (thick red line) and decreasing (thin black line) field sweeps at 20 Oe/s rate. A negative linear slope was subtracted to correct for the diamagnetic contribution from the substrate. The exchange bias field, the horizontal shift of the hysteresis loop from the origin, is −1.6 kOe. The asymmetric reversal is characterized by an initial sharp decrease of magnetization from positive saturation and a slow approach to the negative saturation with an almost negligible (<20 Oe) coercive field. This lack of the coercive field and asymmetric hysteresis loop indicates the presence of reversible rotation of magnetic moments.[22]

The hysteresis loop of the reference sample is compared with the AMR signal of a cross device obtained using two probes (V_{12}) along the unidirectional anisotropy axis (inset of Fig. 1(b)). The AMR was measured at 5 K after 50 Oe field cooling using the earlier cooling protocol. Before field cooling, the easy axis of the cross-junction was determined at 300 K from the AMR angular dependence. The AMR ratio at 5 K is close to ∼1% for both current parallel and perpendicular to the field directions. A −1.6 kOe exchange bias field is obtained from the minimum in AMR curves. The AMR shape, appearance of exchange bias, asymmetric loop shape, and low coercive field are in good agreement with the VSM measurements of the reference. This suggests that the coupling between Ni and FeF_2 was not affected by the lithography.

After initial AMR measurements with the applied field along the unidirectional anisotropy axis (defined as the zero degrees reference position), we perform further measurements at slightly rotated angles (+4° or −4°). The magnetization and AMR at these two different starting points (+4° or −4°) show no significant difference with respect to the zero degree one (Fig. 1(b)). On the other hand, the PHE at +4° is considerably different than at −4 (Fig. 2(a)). Note that the PHE signal was obtained simultaneously with the AMR using the voltage leads which probe the transverse voltage (V_{34}, Fig. 1(b) inset). The absence and presence of significant

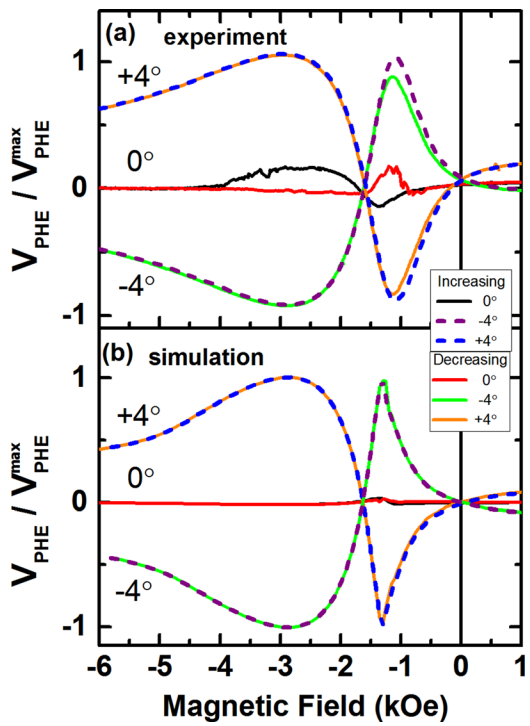

FIG. 2. Normalized PHE signal of the cross junction at 0°, +4°, and −4°. (a) Experimental data and (b) simulation. The PHE was measured from the contacts 3 and 4 (V_{34}) in the inset of Fig. 1(b).

changes in the AMR and PHE geometries for the same device is quite remarkable. These are connected to the slight deviations from the unidirectional anisotropy axes, which induce a preferred initial rotation direction ("chirality") to the magnetic moments.

The differences between AMR and PHE arise from the origin of these two different measurements. Both signals depend on the angle θ, the angle between the current and magnetization direction.[23] The AMR is a function of $\cos^2\theta$, an even function which cannot distinguish between positive and negative θ. In other words, the AMR is insensitive to the rotation direction of magnetic moments and therefore no significant difference is observed for $\pm 4^\circ$. However, the PHE varies as $\sin\theta\cos\theta$, which depends on the rotation direction.[24] Consequently, the opposite PHE at $\pm 4^\circ$ in Fig. 2 are due to the change in rotation direction of the magnetic moments respect to the electrical current I. This change in the rotation direction is induced by the transverse component of the magnetization at $\pm 4^\circ$. For a fixed angle, the rotation direction is always the same and the PHE signal in an increasing and decreasing field sweeps are almost identical.

The above arguments explain the differences in the PHE for slightly different initial conditions, but fail to explain the lack of coercive field and the asymmetric reversal. To explain these, we simulated the magnetization reversal using an incomplete domain wall model. This model accounts for the reversal through rotation of the magnetic moments rather than domain wall nucleation and motion.[25,26] The ferromagnetic layer is assumed to consist of N-planar sub-layers parallel to the FM/AFM interface. The magnetic moment of each sub-layers forms an angle β_i with the reference axis (the easy axis), where $i = 1$ is the first FM sub-layer in contact with the AFM. The maximum angle of the domain wall in the AFM, α, is given by the orientation of nearest AFM spins to the easy axis. The external magnetic field is applied along the easy axis. The total energy of the system is given by

$$E = 2\sqrt{A_{AFM}K_{AFM}}(1-\cos\alpha) - J_{AFM-FM}\cos(\beta_1-\alpha) - J_{FM}\sum_{i=1}^{N-1}\cos(\beta_{i+1}-\beta_i) - K_{FM}\Delta t_{FM}\sum_{i=1}^{N}\cos^2\beta_i - M\Delta t_{FM}H\sum_{i=1}^{N}\cos\beta_i. \quad (1)$$

The first term is the AFM domain wall energy and the second term is the interfacial exchange energy. The other terms represent the FM energy; the exchange coupling between FM sub-layers, the anisotropy energy, and the Zeeman energy of each sub-layer. A_{AFM} and K_{AFM} are the exchange stiffness and anisotropy constant of the AF, respectively. $J_{\mathrm{AFM\text{-}FM}}$ is the exchange coupling constant at the interface, while J_{FM} denotes the exchange coupling constant between adjacent FM sublayers. K_{FM} is the FM anisotropy constant, m_i $(m_i = M_{Ni}\Delta t_{FM})$ is the magnetic moment of each sublayer, and H is the applied magnetic field.[27] The parameters used in the model were: $A_{AFM} = 3.1\times10^{-8}$ erg/cm, $K_{AFM} = 1.35\times10^{8}$ erg/cm^3,[28,29] $J_{AFM-FM} = 0.92$ erg/cm^2, and $J_{FM} = 5.6$ erg/cm^2 were adjusted to fit the M(H) curve. $K_{FM} = 5\times10^{4}$ erg/cm^3 was obtained from the hysteresis loop with the applied field along the hard axis and m_{i} was calculated from the Ni magnetization $M_{Ni} = 485$ emu/cm^3 (Ref. 30) using $m_i = M_{Ni}\Delta t_{FM}$. The thickness of each FM sublayer Δt_{FM} was set to 1 nm. The simulated PHEs (Fig. 2(b)) are obtained using the average magnetization directions of each layer and minimizing the total energy of the system for each external magnetic field during the reversal.

The simulations at $\pm 4^\circ$ reproduce well the experimentally observed fast change in the magnetization approaching the exchange bias field and the slow saturation at negative fields. The asymmetric shape of the PHE arises from incoherent rotation of magnetic moments, i.e., the top most layer rotates first and the others turn sequentially during the reversal.[22] In other words, at saturation, the magnetic moments of each sub plane are all parallel and lay in the plane. The first FM sub layer, in direct contact with the AFM layer is strongly exchange coupled and fixed along the cooling field direction. During reversal, a larger field than the exchange bias is required to overcome this coupling. Due to the short range of the exchange interactions, the AFM-FM exchange coupling strength weakens further from the AFM layer. Therefore, FM layers further from the AFM/FM interface rotate easier than the ones closer. The magnetic moments of each sub planes rotate by a fixed angle with respect to the neighboring plane. Thus, an incomplete domain wall forms along the FM thickness during reversal.

Fig. 3 shows the simulated angular positions of average magnetization for each Ni sublayer at three different fields. The in-depth wall in the Ni layer is quite significant and increases with applied field. For instance, the wall width is 17°, 34°, and 39°, at H = −1.2, −1.6, and −2.2 kOe, respectively. It is important to note that such in-depth domain wall forms even for very thin Ni layer which produces the distinct PHE.

The zero degrees PHE reveals further details of the magnetization reversal process in our prototypical exchange coupled system. At zero degrees, there is no initial preferred rotation direction for all magnetic moments, and therefore, the PHE signal includes both left and right handed rotations.[31] These opposite rotations, produce opposite PHE signals and therefore the average signal is reduced about 85%

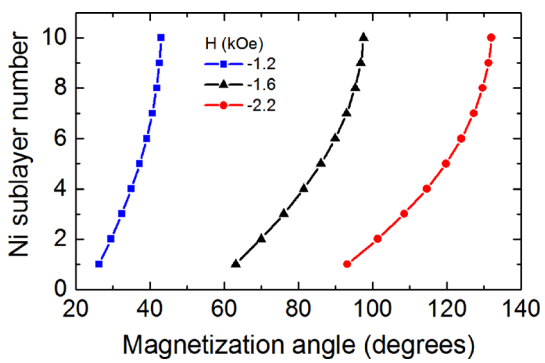

FIG. 3. Angular position of the average magnetization of each sublayer throughout the 10 nm Ni layer at three external fields ($H_{EB} = -1.6$ kOe. Sublayer no. 1 corresponds to the Ni slab in contact with the AFM).

(compared to ±4°). To explain these measurements, we assume the presence of two different directions of pinned moments, which are slightly tilted from the average crystallographic EA in opposite direction. This assumption does not exclude the presence of moments, which are at zero degrees or other possible directions, but it is used to simplify the problem. We further assume that the average distribution of the moments that are aligned in the EA1 direction is slightly higher than in EA2. The simulated PHE curves reproduce the reduction of the signal amplitude at zero degrees although exact details are different. When the maximum magnetic field is applied at zero degrees, Ni magnetization is saturated in this direction. As the magnetic field is reduced, Ni spins rotate towards the local unidirectional anisotropy. One spin population has rotated towards EA1 and the other population has rotated in opposite direction towards EA2. The average PHE signal arises from the sum of these two individual rotations of opposite sign. These results indicate that the high sensitivity of the PHE to the rotation direction of magnetic moments can be used to probe the angular distribution of pinned moments along the AFM easy axis. Further details of this complex reversal mechanism are beyond the scope of this letter.

The preferred rotation direction of the magnetic moments is determined by slight deviations from the well-defined unidirectional anisotropy axis and produce opposite PHE signals. If the magnetic field is applied at a small angle, but larger than the angular distribution of the local unidirectional anisotropy axes, e.g., ±4°, the magnetic moments in each easy axis are forced to follow the same rotation direction (depending on the angle of the applied field). Thus, the PHE signal can be used to determine relative helicity that forms during the reversal in exchange coupled nanojunctions.

In summary, we have shown that a laboratory based PHE measurement allows detection of in-depth helical spin formations in exchange coupled FeF_2/Ni cross junctions. Epitaxial insulating, antiferromagnetic FeF_2 was used to induce a unidirectional anisotropy for the magnetic moments of a ferromagnetic Ni layer. The interfacial exchange coupling produces an in-depth helical spin structure during reversal in the Ni. This helical spin structure and the helicity were confirmed by PHE and simulations using an incomplete domain wall model. An initial rotation direction of magnetic moments can be induced by small angle variations around the unidirectional anisotropy axis and thus control the helicity. Furthermore, PHE reveals complex reversal features due to small deviations of the local unidirectional anisotropy from the crystallographic easy axis. The experiments and simulations are in excellent agreement for all geometries and magnetic fields.

We thank M. Kiwi, D. Altbir, J. G. Ramirez, and C. Monton for the fruitful discussions and critical reading of the manuscript. The work was funded by the Office of Basic Energy Science, U.S. Department of Energy, BES-DMS funded by the Department of Energy's Office of Basic Energy Science, DMR under Grant No. DE FG02 87ER-45332. R.M. acknowledges support from the European Union FP7-IRSES-2012 Grant No. 318901, Spanish MINECO Grant. Nos. FIS2013-45469 and CAS12/00241.

[1]M. N. Baibich, J. M. Broto, A. Fert, F. Nguyen Van Dau, F. Petroff, P. Etienne, G. Creuzet, A. Friederich, and J. Chazelas, Phys. Rev. Lett. **61**(21), 2472 (1988).
[2]S. D. Bader, Rev. Mod. Phys. **78**(1), 1 (2006).
[3]A. Fert, V. Cros, and J. Sampaio, Nat. Nanotechnol. **8**(3), 152 (2013).
[4]E. E. Fullerton, J. S. Jiang, M. Grimsditch, C. H. Sowers, and S. D. Bader, Phys. Rev. B: Condens. Matter **58**(18), 12193 (1998).
[5]R. Morales, Z.-P. Li, O. Petracic, X. Batlle, I. K. Schuller, J. Olamit, and K. Liu, Appl. Phys. Lett. **89**, 072504 (2006).
[6]T. N. Anh Nguyen, R. Knut, V. Fallahi, S. Chung, Q. Tuan Le, S. M. Mohseni, O. Karis, S. Peredkov, R. K. Dumas, C. W. Miller, and J. Åkerman, Phys. Rev. Appl. **2**(4), 044014 (2014).
[7]S. Roy, M. R. Fitzsimmons, S. Park, M. Dorn, O. Petracic, I. V. Roshchin, Z.-P. Li, X. Batlle, R. Morales, A. Misra, X. Zhang, K. Chesnel, J. B. Kortright, S. K. Sinha, and I. K. Schuller, Phys. Rev. Lett. **95**(4), 047201 (2005).
[8]H. Thomas, R. Rohlsberger, K. Schlage, and T. Klein, J. Magn. Magn. Mater. **282**, 329 (2004).
[9]M. Uchida, Y. Onose, Y. Matsui, and Y. Tokura, Science **311**(5759), 359 (2006).
[10]S. Mühlbauer, B. Binz, F. Jonietz, C. Pfleiderer, A. Rosch, A. Neubauer, R. Georgii, and P. Böni, Science **323**(5916), 915 (2009).
[11]T. R. McGuire and R. I. Potter, IEEE Trans. Magn. **11**(4), 1018 (1975).
[12]E. Dan Dahlberg, K. Riggs, and G. A. Prinz, J. Appl. Phys. **63**(8), 4270 (1988).
[13]A. Tillmanns, S. Oertker, B. Beschoten, G. Güntherodt, C. Leighton, I. K. Schuller, and J. Nogués, Appl. Phys. Lett. **89**, 202512 (2006).
[14]T. Pokhil, R. Chantrell, C. Hou, and E. Singleton, J. Magn. Magn. Mater. **272–276**, E849 (2004).
[15]V. Dinh Ky, Phys. Status Solidi B **26**(2), 565 (1968).
[16]A. Schuhl, F. Nguyen Van Dau, and J. R. Childress, Appl. Phys. Lett. **66**(20), 2751 (1995).
[17]F. Montaigne, A. Schuhl, F. Nguyen Van Dau, and A. Encinas, Sens. Actuators, A **81**(1–3), 324 (2000).
[18]C. D. Damsgaard, S. C. Freitas, P. P. Freitas, and M. F. Hansen, J. Appl. Phys. **103**, 07A302 (2008).
[19]L. Ejsing, M. F. Hansen, A. K. Menon, H. A. Ferreira, D. L. Graham, and P. P. Freitas, Appl. Phys. Lett. **84**(23), 4729 (2004).
[20]Z. Ge, W. L. Lim, S. Shen, Y. Y. Zhou, X. Liu, J. K. Furdyna, and M. Dobrowolska, Phys. Rev. B: Condens. Matter **75**(1), 014407 (2007).
[21]Y. S. Huang, C. C. Wang, and A. O. Adeyeye, J. Appl. Phys. **100**, 013909 (2006).
[22]Z.-P. Li, O. Petracic, R. Morales, J. Olamit, X. Batlle, K. Liu, and I. K. Schuller, Phys. Rev. Lett. **96**(21), 217205 (2006).
[23]D. A. Thompson, L. T. Romankiw, and A. Mayadas, IEEE Trans. Magn. **11**(4), 1039 (1975).
[24]Note that the angular dependence of both AMR and PHE signals become same for 45°. Therefore, a very specific choice of the AMR geometry at 45° to the current direction could be used to sense the magnetization rotation direction as well. (S. Brems, H. Liu, K. Temst, and C. V. Haesendonck, Phys. Rev. B: Condens. Matter **88**, 214427 (2013)).
[25]D. Mauri, H. C. Siegmann, P. S. Bagus, and E. Kay, J. Appl. Phys. **62**(7), 3047 (1987).
[26]M. Kiwi, J. Mejía-López, R. D. Portugal, and R. Ramírez, EPL **48**(5), 573 (1999).
[27]R. Morales, A. C. Basaran, J. E. Villegas, D. Navas, N. Soriano, B. Mora, C. Redondo, X. Batlle, and I. K. Schuller, Phys. Rev. Lett. **114**(9), 097202 (2015).
[28]J. Nogués, D. Lederman, T. J. Moran, I. K. Schuller, and K. V. Rao, Appl. Phys. Lett. **68**(22), 3186 (1996).
[29]Z.-P. Li, C. W. Miller, I. V. Roshchin, and I. K. Schuller, Phys. Rev. B: Condens. Matter **76**(1), 014423 (2007).
[30]C. Kittel, *Introduction to Solid State Physics*, 8th ed. (Wiley, Hoboken, NJ, 2005).
[31]Note that the AMR measurements probe the same reversal mechanism. However, only PHE can distinguish both left and right handed rotations and therefore produces a complete unique feature.